Extreme-ultraviolet spectral purity and magnetic ion debris mitigation by use of low-density tin targets

S. S. Harilal, M. S. Tillack, Y. Tao, and B. O'Shay

Center for Energy Research, University of California, San Diego, 9500 Gilman Drive, La Jolla, California 92093-0438

R. Paguio and A. Nikroo

General Atomics, San Diego, California 92186

Received December 13, 2005; revised January 29, 2006; accepted January 30, 2006; posted February 16, 2006 (Doc. ID 66615)

We investigate the extreme-ultraviolet (EUV) emission from targets that contain tin as an impurity and the advantages of using these targets for ion debris mitigation by use of a magnetic field. The EUV spectral features were characterized by a transmission grating spectrograph. The in-band EUV emission energy was measured with a calorimeter of absolute calibration. The ion flux coming from the plume was measured with a Faraday cup. Our studies indicate that 0.5% Sn density is necessary to obtain a conversion efficiency very close to that of full-density Sn. The use of Sn-doped low-Z targets provides a narrower unresolved transition array and facilitates better control of energetic ions in the presence of a moderate magnetic field of 0.64 T.

OCIS codes: 300.6560, 350.5400.

Extreme-ultraviolet lithography (EUVL) at 13.5 nm is a leading candidate for next-generation high-volume patterning.[1] The essential requirement for this technology is to have a reliable, clean, and powerful light source near 13.5 nm. Laser-produced tin plasma has a strong potential to be the future extreme-ultraviolet (EUV) light source and offers higher conversion efficiency (CE) than xenon-based sources.[1–3] However, apart from attainment of high CE, decreasing debris from the source and hence enhancing optics lifetime and spectral purity are the main concerns that are being addressed by the developers of light sources. The biggest concern is that fast ions from the plasma are expected to significantly damage the collector mirror by-means of ion-induced mixing of the multilayer mirror, by etching and implantation of the multilayer mirror's coating, which is located near the EUV light source.[4] Consequently, various methods for controlling the debris from plasma, including the introduction of tape targets,[5] ambient gas for moderating the species,[6] and foil traps,[7] cavity confinement,[3] application of electrostatic repeller fields,[8] and magnetic fields,[9,10] have been proposed. Another way to reduce debris is to use mass limited targets, for which the numbers of Sn atoms are just enough to provide bright unresolved transition array (UTA) emission.[8]

Opacity effects significantly influence the EUV spectral energy from laser-produced Sn plasma. Fujikoa *et al.*[11] studied opacity effects and suggested that one can control the optical thickness of Sn plasma by changing the initial target density. One of the most effective ways to accomplish this is to use Sn atoms as a measurable impurity in an EUVL target. In this Letter we report the advantages of using low-Z targets with Sn as an impurity as well as the effective mitigation of ion debris by use of a magnetic field.

For producing plasma, 1064 nm, 10 ns FWHM pulses from a Nd:YAG laser were used. The target was mounted in a vacuum chamber with a base pressure of $\sim 10^{-6}$ Torr. The 60 μm diameter focal spot was measured with an optical imaging technique and remained unchanged during the experiment. The EUV emission from the plasma was measured with a transmission grating spectrograph equipped with a 10,000 line/mm grating and a backilluminated x-ray CCD camera. A Jenoptik EUV calorimeter was used for measuring the CE of the in-band radiation at 13.5 nm with 2% bandwidth. The EUV calorimeter and the transmission grating spectrograph were placed at 45° with respect to the laser beam. As the EUV plasma emission has an approximately hemispherical symmetry,[12] we simply integrated the output from the energy monitor over a 2π solid angle to obtain CE.

The ion emission from the plume was monitored with a Faraday cup. The ambient magnetic field was supplied by an assembly of two permanent magnets (B_{max}=1.2 T) mounted in a steel core, creating a uniform field configuration over a volume of 5 cm $\times$2.5 cm$\times$1.5 cm. The maximum magnetic field was 0.64 T and was nearly uniform along the direction of plume expansion.[13]

To fabricate the Sn-doped foam bead targets, the required amount of SnO_2, which contains 78.8% of Sn by mass, is dispersed into a resourcinol formaldehyde (density, 100 mg/cm^3) solution and dried. EUV spectral measurements with various concentrations of Sn showed that the brightness of the UTA was more-or-less constant when the Sn density dropped from 100% to 0.5%, indicating that plasma is optically thick to 13.5 nm. A typical UTA recorded from a full-density Sn target and 0.5% Sn doped foam targets is shown in Fig. 1. The UTA emission is concentrated near 13.5 nm and arises from $4p^64d^n-4p^54d^{n+1}$

0146-9592/06/101549-3/$15.00

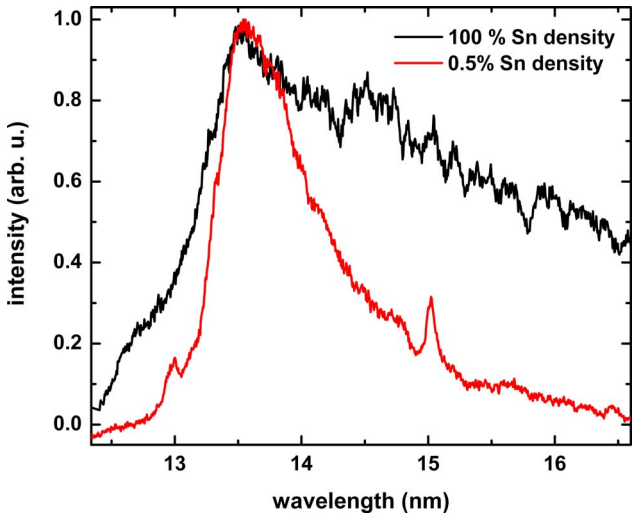

Fig. 1. (Color online) UTA obtained from full-density and 0.5% density Sn. The UTA spectrum from Sn-doped foam targets showed distinct narrowing. Both spectra were recorded with a laser intensity of 4×10^{11} W cm^{-2}.

$+4p^6 4d^{n-1}4f$ transitions of various Sn ions ranging from Sn^{6+} to Sn^{14+}, with occupancy in the range $n=2-8$, as shown by Cummins *et al.*[14] The spectral features of Sn-doped foam targets also contained oxygen emission lines. They are identified as O^{5+} lines at 12.99 nm ($2p-4d$) and 15.00 nm ($2s-3p$).

Compared with that of a solid Sn slab, UTA emission from Sn-doped foam targets showed reduced continuum emission and a narrowed spectrum peaked at 13.5 nm. Fujioka *et al.*[11] observed similar narrowing of the UTA by using low-density targets and attributed it to a reduction of satellite emission from multiply excited Sn ions and to less opacity broadening during the radiation transport. Aota *et al.*[15] also reported a narrower UTA profile from a cavity-confined Sn plasma. Theoretical calculations showed[14,16] that the core Sn ions that contribute to the UTA at 13.5 nm range from Sn^{10+} to Sn^{13+}, while lower-charged species ($Sn^{6+}-Sn^{9+}$) emit at the longer-wavelength side of the UTA (>14 nm). The UTA from the 0.5% Sn targets compared with that from 100% Sn showed a reduction of emission at a wavelength of >14 nm. This indicates that a decrease in Sn density leads to quenching of lower ionization states.

Figure 2 shows the dependence of CE on laser intensity. The CE of full-density Sn was found to peak near 4×10^{11} W/cm^2 and attained a maximum of $2.04\pm0.1\%$, while the highest CE obtained for 0.5% density Sn was $1.95\pm0.1\%$ and peaked at 8×10^{11} W/cm^2. This shows that a small density of Sn is necessary to produce CE close to that of full-density Sn. White *et al.*[16] reported that CE measurement is highly sensitive to the charge-state distribution of Sn. According to Fig. 2, higher laser intensity is required for reaching the same $\langle Z\rangle$ in the low-Sn-density target as in the full-Sn-density target. From Fig. 1 one can infer that, for the same peak intensity, the measured CE for the 0.5% Sn density target has to be smaller than for the 100% Sn density target because of the steeper slope of the UTA feature on the low-wavelength side.

The ion-debris measurements were carried out in the presence and in the absence of a magnetic field by use of a Faraday cup placed 15 cm from the target and at an angle of approximately 12° with respect to the target normal. It should be noted that the distribution of ions in a laser-created plasma is best approximated by a single charge-dependent $\cos^n$ function for which the value of n increases with the charge state and decreases with the atomic mass.[17] Figure 3 shows a comparison of signals of Faraday cups between full-density Sn and 0.5% Sn-doped foam targets in the presence and in the absence of a transverse magnetic field of 0.64 T. For applying a magnetic field, a target placed a distance of 1 cm from the pole edges resulted in a uniform magnetic field along the plume's direction of expansion.[13]

The kinetic energy distribution of the Sn ions showed energies of as much as 5 keV, with a peak ion flux at 1.2 keV. In the presence of the magnetic field the Sn ions have slow down considerably but are not fully mitigated. It is also worth noting that the collector charge yield increased considerably in the presence of the B field, maybe because of the deflection of ions by the field. The ions coming out from the foam targets have a maximum probable velocity of $\sim1\times10^7$ cm/s, which is considerably larger than the expansion velocity of Sn ions from pure Sn targets ($\sim4.3\times10^6$ cm/s). But the magnetic field showed more influence in controlling light ions, and from Fig. 3 it can be seen that the ion flux is reduced by more than 1 order of magnitude for the foam target. Optical time-of-flight studies showed that neutrals can also be effectively controlled by the magnetic field due to confinement of the plume.[9,13]

When a plume expands into a B field, the plume's behavior is controlled mainly by thermal beta[18] ($\beta_t=2\mu_0 nkT/B^2$) and by directed beta ($\beta_d=\mu_0 nmv^2/B^2$), where n, T, and v are the density, temperature, and velocity, respectively. Our analysis showed that ther-

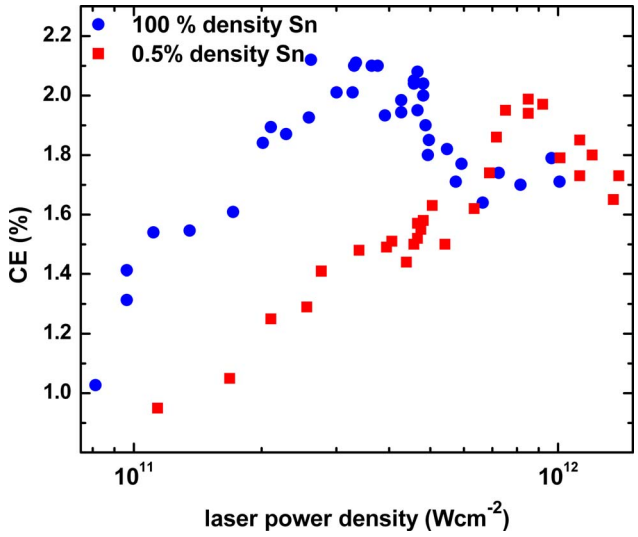

Fig. 2. (Color online) Estimated CE for a full-density Sn and a 0.5% Sn-doped foam target at various laser intensities.

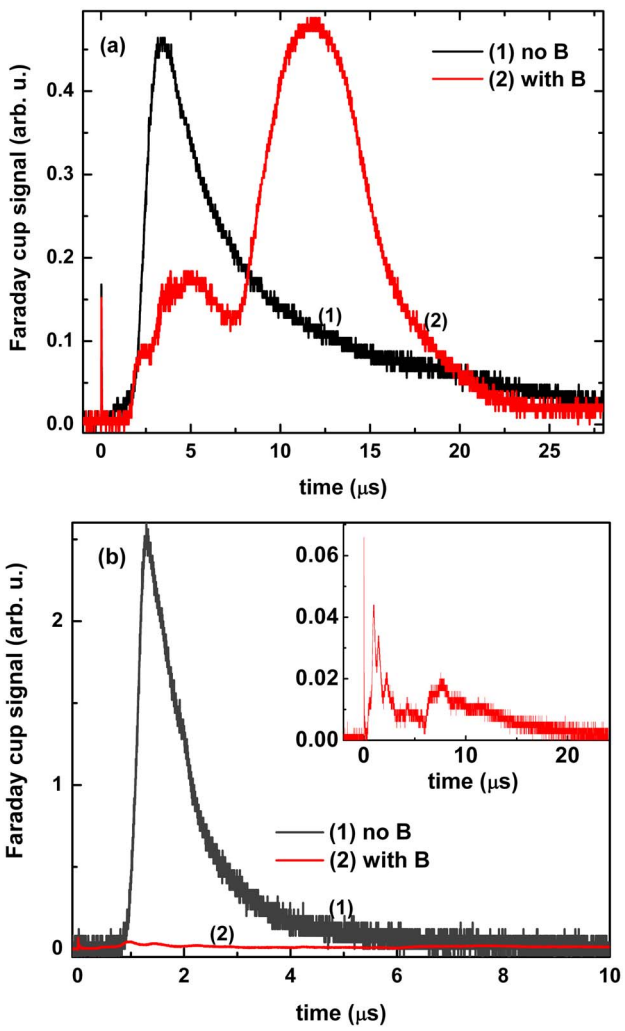

Fig. 3. (Color online) Typical ion time-of-flight signals recorded for (a) full density and (b) 0.5% density Sn in the presence and in the absence of a magnetic field. A magnified version of the time-of-flight profile obtained from 0.5% Sn in the presence of a magnetic field is given in the inset of (b).

mal beta (β_t) of the plasma approaches unity ~100 ns after formation of the plasma. After the initial conversion of thermal energy to directed energy, directed β (β_d) becomes an important parameter. In the early phase of the plume's expansion, β_d is of the order of a few thousand, indicating that the plume is experiencing diamagnetic expansion. The laser-produced plasma's diamagnetic cavity (magnetic bubble) expands until the total excluded magnetic energy becomes comparable with the total plasma energy.[13] Spectroscopic studies in the visible[19] indicate that, at late stages, the bulk ion component is Sn^+, whose Larmor radius is ~3.5 cm, and its value decreases with increasing charge state. The Sn-doped foam targets contain several elements with various atomic percentages [Sn (1.8%), O (17.2%), C (27%), and H (54%)], showing that the main contribution is from low-Z elements. Even though Faraday cup measurements showed nearly double the velocity for ions emanating from Sn-doped foam targets compared with those from solid Sn, β_d was found to be much lower for Sn-doped foams because of the lower average mass.

In conclusion, we have reported the effectiveness of using a tin-doped foam target for ion mitigation by using a transverse magnetic field. A moderate magnetic field of 0.64 T was found to be effective for mitigating energetic ions by more than 1 order of magnitude when Sn was doped as an impurity in a low-Z target, while the field slowed down only Sn ions coming out from the full-density Sn plasma. The low-density Sn targets also provided high spectral purity by having a narrower UTA spectrum. The CE measurements showed that 0.5% Sn density is necessary to produce a CE that is obtained with full-density Sn.

S. Harilal's e-mail address is sharilal@ucsd.edu.

References

1. B. Marx, Laser Focus World **39**(4), 34 (2003).
2. R. C. Spitzer, R. L. Kauffman, T. Orzechowski, D. W. Phillion, and C. Cerjan, J. Vac. Sci. Technol. A **11**, 2986 (1993).
3. T. Tomie and T. Aota, Phys. Rev. Lett. **94**, 015004 (2005).
4. J. P. Allain, A. Hassanein, M. Nieto, V. Titov, P. Plotkin, E. Hinson, and C. Chrobak, in Proc. SPIE **5751**, 1110 (2005).
5. S. J. Haney, K. W. Berger, G. D. Kubiak, P. D. Rockett, and J. Hunter, Appl. Opt. **32**, 6934 (1993).
6. F. Flora, L. Mezi, C. E. Zheng, and F. Bonfigli, Europhys. Lett. **56**, 676 (2001).
7. J. Pankert, R. Apetz, K. Bergmann, A. List, M. Loeken, C. Metzmacher, W. Neff, and S. Probst, in Proc. SPIE **5751**, 260 (2005).
8. M. Richardson, C. S. Koay, K. Takenoshita, C. Keyser, and M. Al-Rabban, J. Vac. Sci. Technol. A **22**, 785 (2004).
9. S. S. Harilal, B. O'Shay, and M. S. Tillack, J. Appl. Phys. **98**, 036102 (2005).
10. G. Niimi, Y. Ueno, K. Nishigori, T. Aota, H. Yashiro, and T. Tomie, in Proc. SPIE **5037**, 370 (2003).
11. S. Fujioka, H. Nishimura, T. Okuno, Y. Tao, N. Ueda, T. Ando, H. Kurayama, Y. Yasuda, S. Uchida, Y. Shimada, M. Yamaura, Q. Gu, K. Nagai, T. Norimatsu, H. Furukawa, A. Sunahara, Y. Kang, M. Murakami, K. Nishihara, N. Miyanaga, and Y. Izawa, in Proc. SPIE **5751**, 578 (2005).
12. Y. Tao, F. Sohbatzadeh, H. Nishimura, R. Matsui, T. Hibino, T. Okuno, S. Fujioka, K. Nagai, T. Norimatsu, K. Nishihara, N. Miyanaga, Y. Izawa, A. Sunahara, and T. Kawamura, Appl. Phys. Lett. **85**, 1919 (2004).
13. S. S. Harilal, M. S. Tillack, B. O'Shay, C. V. Bindhu, and F. Najmabadi, Phys. Rev. E **69**, 026413 (2004).
14. A. Cummings, G. O'Sullivan, P. Dunne, E. Sokell, N. Murphy, and J. White, J. Phys. D **38**, 604 (2005).
15. T. Aota, H. Yashiro, Y. Ueno, and T. Tomie, in Proc. SPIE **5037**, 742 (2002).
16. J. White, P. Hayden, P. Dunne, A. Cummings, N. Murphy, P. Sheridan, and G. O'Sullivan, J. Appl. Phys. **98**, 113301 (2005).
17. A. Thum-Jager and K. Rohr, J. Phys. D **32**, 2827 (1999).
18. B. H. Ripin, E. A. McLean, C. K. Manka, C. Pawley, J. A. Stamper, T. A. Peyser, A. N. Mostovych, J. Grun, A. B. Hassam, and J. Huba, Phys. Rev. Lett. **59**, 2299 (1987).
19. S. S. Harilal, B. O'Shay, M. S. Tillack, and M. V. Mathew, J. Appl. Phys. **98**, 013306 (2005).